MECHANICAL PERFORMANCE OF REPAIRED SANDWICH PANELS: EXPERIMENTAL AND NUMERICAL INVESTIGATIONS

Ghazali, E, Dano, M-L*, Gakwaya, A
Mechanical Engineering Department, Laval University, Quebec (G1V 0A6), Canada
* Corresponding author (**Marie-Laure.Dano@gmc.ulaval.ca**)

Keywords: *Sandwich structures, bonded repair, finite element analysis*

ABSTRACT

Stepped-scarf patch repairs of sandwich honeycomb structures can offer a good alternative easier to perform than tapered scarf repairs that are widely used for primary aerospace applications. This study investigates the effect of different joint geometrical parameters on stress distribution in the adhesive bondline and on the ultimate load of repaired sandwich panels. Both linear elastic and non-linear elastoplastic with failure criterion analyses were conducted to perform a parametric study focusing on the effects of scarf angle, number of plies and the addition of an overply (overlap length). Results show that step-scarf joints have an important sensitivity to the thickness of repaired skins. The use of an overply provides protection to the free ends of the adhesive joint and increases the strength recovery of the repaired structure.

1 INTRODUCTION

Adhesively bonded joints are increasingly being used nowadays in different industry fields and especially in aerospace industry for its advantages in maintaining aerodynamic performance and in ensuring uniform stress distribution. However, to insure the highest strength recovery of the repaired structure, different parameters such as the scarf angle, the lay-up, the adherend thickness, etc., should be taken into account for an optimal repair.

Different experimental studies and finite-element analyses were carried out to study the behaviour of repaired sandwich panels under different static loads. Mahdi et al. [1-3] used 2D and quasi-3D finite-element models to predict the performance of both pristine and scarf repaired sandwich panels subjected to static and fatigue four-point bending loads. Numerical simulation results showed a good correlation in terms of stiffness prediction of both the undamaged and the repaired coupons. However, the ultimate load prediction was problematic and did not show a good correlation with experiments. Campilho et al. [4] developed a 2D cohesive damage model to study the performance of repaired sandwich panels under four-point bending loads. For overlap joints, they concluded that the repair strength increases as a function of the overlap length and that the strength increases with lower scarf angles in the case of scarf joints. The compressive behaviour of repaired sandwich panels was investigated by Liu et al [5]. Both experiments and finite-element analyses were conducted to study the influence of repair variables on the quality of the repair. A progressive damage model was developed and a good correlation between experimental and numerical results was obtained. On the other hand, experimental tests were also conducted by Tomblin et al. [6-7] to study the effects of different process parameters on the repair quality of sandwich panels. A damage tolerance analysis on sandwich structures was also included in their study. As a conclusion of their work, a methodology for the repair process and for damage tolerance design tools of sandwich structures were developed. A recent study from Zhang et al. [8] investigated the mechanical performance of open-hole damage and circular scarf repair honeycomb sandwich panels under compressive loads. A 3D finite-element model was also developed. A failure criteria based on Hashin criterion with a progressive damage evolution was included for the unidirectional composite skins. The adhesive layer was modeled using cohesive elements. The honeycomb core was considered as an elastic-plastic material. A good

agreement was found in terms of ultimate failure load and damage shape between the experimental and numerical results. Another finding of this work is that the structure strength increases with the decrease of scarf angle and that the optimum number of overplies is one that allow to reach the highest strength. In the above-mentioned research works, focus was on scarf-scarf repair modelling using cohesive zone elements for the adhesive bondline. However, this modelling technique is not suitable to model a scarf-stepped repair configuration which is widely used in practice. Simplifying a scarf-stepped configuration by a scarf-scarf configuration may lead to inaccurate predictions of stress distribution. Also most of the above mentioned research works conduct parametric studies using finite-element analysis without correlating numerical predictions with experimental results.
The aim of this paper is thus to investigate the tensile behavior of cocured bonded flush scarf-stepped repair joints for primary structure sandwich panels through numerical methods. Here, a parametric study is conducted to determine the influence of the scarf angle, the number of plies, and the use of an overply (overlap length) on the strength recovery of the repaired specimens. First, a 2D elastic linear model will be used to determine the stress distribution along the bondline. Then, the 2D model will be modified and an elastic-plastic model for the adhesive will be taken into account to determine the ultimate stress failure of different repair configurations. A comparison of the baseline model predictions with experimental results is also presented.

2 GEOMETRY AND MATERIAL MODELS DETAILS

The following subsections describe the model geometry, the boundary conditions, the finite-element mesh and the materials models used in the finite-element analysis of the repair joint of sandwich honeycomb panels.

2.1 Model Geometry

The repaired sandwich panels, considered in our experimental studies, have a double step-scarf joint, where the repair was carried out on the tool facesheet. The panels are 335 mm long, 102 mm wide and 20.5 mm thick. They are composed of an over-expanded Nomex honeycomb core with a 19 mm thickness on which two four-ply carbon-epoxy skins were bonded. The skin is made with an out-of-autoclave plain weave prepreg (CYCOM 5320 T650 PW from Cytec Engineering Materials). The ply stacking sequence for the inner facesheet, also called the tool facesheet, is a [(+45/-45)/ (0/90)/ (-45/+45)/ (90/0)]. The outer facesheet, also called the bag facesheet, has the same lay-up as the inner one. The patch repair has also the same lay-up as the parent structure. The repair joint was considered symmetric. As such, only half the longitudinal cross-section was modeled (Figure 1) using a two-dimensional model with plane strain conditions. The repair patch was bonded to the parent structure by an adhesive film placed along a taper area.

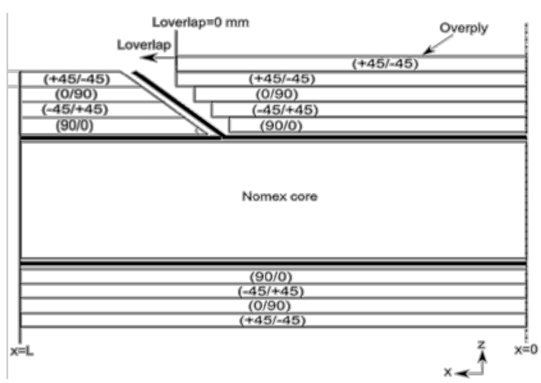

Figure 1 : Symmetric cross-section of double scarf-stepped repair

2.2 Boundary Conditions and Mesh

The boundary conditions are defined as follow. On the left edge (x=L), a total displacement, as measured from the experiment, was applied and, on the right edge (x=0), symmetric boundary conditions were imposed. Each single woven ply and the adhesive film were discretized through the thickness using one and four elements respectively. The adhesive film along the joint as well as between the two skins and the core was modelled too. The Nomex honeycomb core was also discretized through thickness using five elements.

2.3 Materials Models

The finite-element software packages ABAQUS/Standard and ABAQUS/Explicit [9] were used to study the mechanical response of the repaired sandwich panels under tensile loading. Here two types of analysis were conducted. First, an elastic analysis with isotropic elastic behaviour of the adhesive was performed in order to determine the stress distribution along the bondline. The second analysis took into account the von Mises plasticity with a shear failure criterion for the adhesive bondline to predict the mechanical behaviour until failure of the repaired panels [10]. Moreover, the composite skins were modeled as an orthotropic elastic material with a consideration of a maximum fiber deformation criterion for the failure prediction. For both analyses, the honeycomb core was considered as an equivalent orthotropic elastic material. The mechanical properties of the composite material used for the sandwich panels are summarized in Table 1, those of the adhesive film are indicated in Table 2 and those of the Nomex honeycomb core are listed in Table 3.

E_1[GPa]	E_2 [GPa]	E_3 [GPa]	G_{12} [GPa]	ν_{12}	t_p [mm]
64.6[a]	64.6[a]	10[b]	4.9[a]	0.047[a]	0.19

[a] experimentally measured, [b] assumed

Table 1: Mechanical properties of the plain weave composite material

E [GPa]	G [GPa]	ν	τ_y [MPa]
2.024	0.770	0.3	30

Table 2 : Mechanical properties of the FM300-2M adhesive [11]

E_1[MPa]	0.089[a]	G_{12} [MPa]	25.6[b]	ν_{12}	0.263[b]
E_2 [MPa]	30.30[a]	G_{13} [MPa]	21.1[c]	ν_{13}	0.223[b]
E_3 [MPa]	185[a]	G_{23} [MPa]	55.5[c]	ν_{23}	0.029[b]

[a] experimentally measured, [b] taken from published literature [4], [c] provided in material sheets [12]

Table 3: Mechanical properties of the Nomex honeycomb core

3 PARAMETRIC STUDY

A parametric study was performed by varying four geometrical design parameters of the repaired joint: the step-scarf angle, the number of plies and the length of the overlap of the overply. These parameters are listed in Table 4 and the baseline values are shown in Table 5. The main objective of this study is to investigate the influence of these parameters on the stress distribution along the adhesive bondline. For that purpose, shear and peel stresses were evaluated in the middle of the bondline. The peel and shear stresses were normalized by the applied stress, σ_x, to allow the comparison of the relative magnitude as follow:

$$\frac{\tau_{12}}{\sigma_x} X1000 \tag{1}$$

$$\frac{\sigma_{22}}{\sigma_x} X1000 \tag{2}$$

The second objective of this study is to determine the ultimate stress of the repaired structure and to compare it with the one of the pristine panel. The ultimate stress was evaluated using:

$$\sigma^{ult} = \frac{P^f}{2bt_f} \tag{3}$$

where P^f is the ultimate failure load, t_f is the facesheet thickness and b is the panel width.

Parameter	Value
Step-scarf angle α (°)	1.5-15
Number of plies	2, 4 and 8
Overply lay-up	[(+45/-45)]
Overply: overlap length [mm]	0-5-10-15

Table 4 : Parametric model details

Parameter	Value
Step-scarf angle α (°)	3°
Adhesive thickness [mm]	0.25
Ply thickness [mm]	0.19
Number of plies	4
Overply lay-up	no overply
Overply: overlap length [mm]	no overply
Skin lay-up	[(+45/-45)/ (0/90)/ (-45/+45)/ (90/0)]

Table 5: Baseline model values

4 RESULTS AND DISCUSSIONS

4.1 Effect of the Scarf Angle

In this section, the influence of various scarf angles (from 1.5° to 15°) for a step-scarf bonded repair for the same baseline lay-up and number of plies is considered. First, the effect on the stress distribution along the bondline will be discussed. Then, to further study the influence of the scarf angle on the tensile strength, finite-element analyses with failure criteria will be conducted using models with different scarf angles. The ultimate stress variation as a function of the scarf angle will be presented.

4.1.1 *Shear and Peel Stresses Distribution along the Bondline*

Figures 2(a) and 2(b) compare the shear and the peel stresses distributions along the normalized adhesive bondline for different scarf angles, respectively. As expected, peak stresses occur in the vicinity of (0/90) plies and the stress distribution varies from one ply to another unlike homogenous adherend. It can be also seen that the bondline stresses are very sensitive to the scarf angle variation. These results are in accordance with conclusions of previous works [13-15] conducted on monolithic composite repairs. The repair joint with a 1.5° scarf angle shows the lowest shear stress distribution when compared to other scarf repair angles. The highest peak stresses are observed for the 15° scarf angle. Therefore, failure would be likely to occur sooner for a 15°scarf joint than for a 1.5° scarf repair.

4.1.2 *Failure Load*

Figure 3 shows the evolution trend of the ultimate tensile stress with the increase of the scarf angle. Experimental results [10] are also added for comparison and validation of the model. For scarf angles between 3° and 7°, the ultimate stress decreases only very slightly. For scarf angles below 3°, the strength increases exponentially with angle reduction. However, for scarf angles over 7°, it decreases drastically. This phenomenon is related to the decrease of the step length with the increase of the angle, which induces increase in the peel and shear peak stresses at the bondline ends and in the neighborhood of the stepped plies. For the failure mode, it was observed that the failure occurs in the adhesive film for angles from 1.5° to 15°. The higher strength recovery was obtained for the 1.5° scarf angle. A good agreement in the ultimate stress and failure morphology was found between the experimental results and the finite element predictions for angles from 3° to 7°.

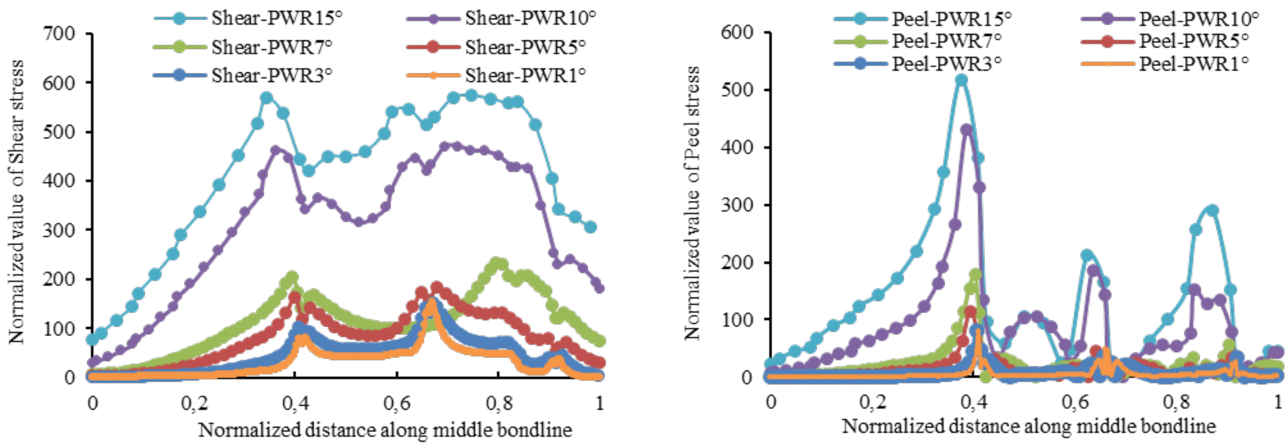

(a) Shear stress distribution

(b) Peel stress distribution

Figure 2 : Shear and peel stresses distribution for different step-scarf angles in the middle of the adhesive bondline

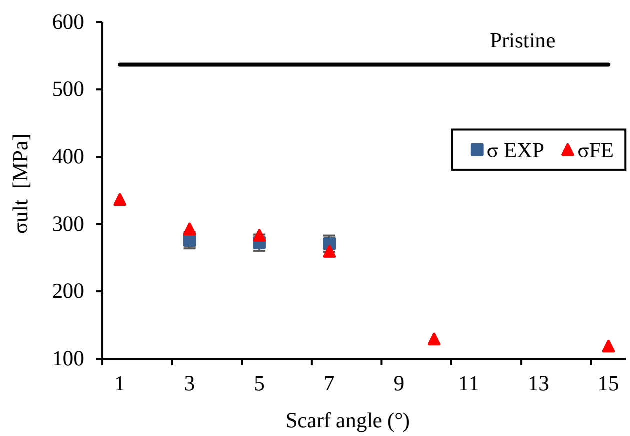

Figure 3 : Repair ultimate stress for different scarf angles

4.2 Effect of Overply-Overlap Length

Here, the effect of a (+45/-45) overply on the 3°-scarf joint model with the baseline parameters is investigated. The overply thickness is made with the same plain weave composite material as the parent and the patch plies. Here, the overlap length (L overlap) varied from 0 mm to 15 mm, as shown in Figure 1. The same boundary conditions and displacement were applied as for the baseline model.

4.2.1 *Shear and Peel Stresses Distribution along the Bondline*

From the results shown in Figure 4, it can be observed that when the overlap length is equal to zero (0 mm), the peel and shear peak stresses are still important. For an overlap length equal to 5 mm, a drop in both shear and peel stresses peak can be seen. However, since for this overlap length, the free edge of the adhesive is not completely covered, a step is added by the overply. This step induces an additional peak in the shear and peel stress distribution at the beginning of the bondline. This additional peak disappears with an overlap length of 10 mm and an important drop in the shear and peel stresses along the bondline can be clearly seen. Increasing the overlap length from 10 mm to 15 mm is observed to have little effect on the stress distribution along the adhesive bondline. The addition of an overply has also a clear effect on the peak stresses in a monolithic scarf joint repair. However, no significant advantage was observed by increasing the number of overply in the reducing of the peak stresses [13]. A critical overlap length of 5 mm was also found for stepped flush repair joint from the work done by Bendemra et al [15] for stepped-lap joints in monolithic repair patches.

4.2.2 *Failure Load and Finite Element Validation*

Figure 5 shows the evolution of the ultimate stress in the facesheet as a function of the overply length. It can be clearly seen that the addition of an overply has an important effect on the ultimate stress. An increase of the strength is observed as the overlap length increases. It can be also seen that a length of 10 mm can be considered as a critical value. Passed this value, no major effect on the ultimate stress has been observed. A higher strength recovery is obtained in comparison with the no overply configuration. This recovery reaches about 90% of the pristine value. A change in the failure mode was observed too. The failure occurs no more in the adhesive bondline as for the baseline configuration but in the composite plies. In order to validate the numerical predictions for the overply effect, tensile tests have been conducted in accordance with the work discussed in a previous paper [10]. Three specimens with one (+45/-45) overply and an overlap length of 10 mm were tested. The measured strength is indicated in Figure 5. As can be seen, the numerical results are slightly higher than the experimental results. However, they are in good agreement and confirm the important effect of the addition of an overply on the strength recovery.

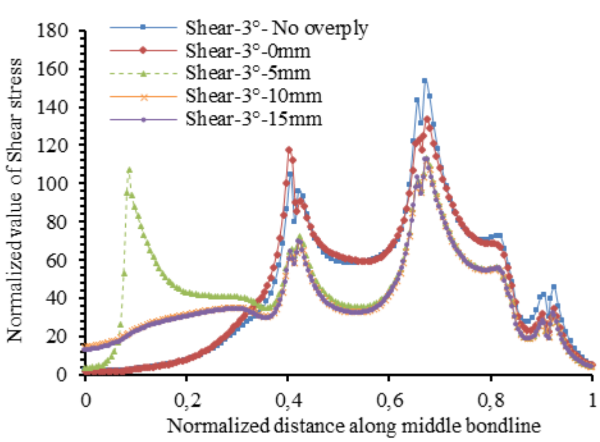

(a) Shear stress distribution

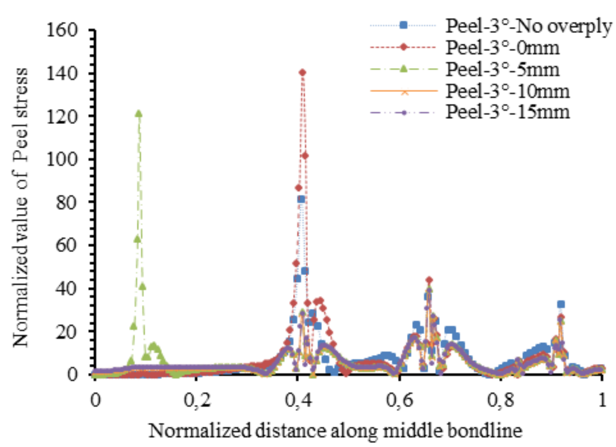

(b) Peel stress distribution

Figure 4 : Shear and peel stresses distribution as a function overlap length in the middle adhesive bondline for a 3° 4-ply model

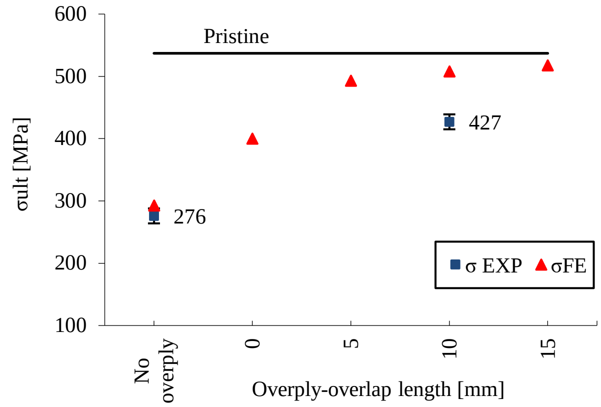

Figure 5 : Repair strength prediction as function of the overlap length (4-ply skin, 3°scarf angle)

4.3 *Effect of Number of plies*

To highlight the effect of increasing the number of plies (adherend thickness) on the stress distribution along the adhesive bondline and on the strength recovery, repaired sandwich panels with 2-ply skins, 4-ply skins and 8-ply skins were modelled. The lay-up sequence for each model is as follow:

- 2-ply skin: [(+45/-45)/ (0/90)]
- 4-ply skin: [(+45/-45)/ (0/90)/ (-45/+45)/ (90/0)]
- 8-ply skin: [(+45/-45)/ (0/90)/ (-45/+45)/ (90/0)/ (+45/-45)/ (0/90)/ (-45/+45)/ (90/0)]

To maintain a ply-by-ply match, a change in number of plies was applied equally to the parent part and the patch. The same plain weave composite material was used too and the boundary conditions are similar to the baseline configuration.

4.3.1 *Shear and Peel Stresses Distribution along the Bondline*

The shear and peel stresses distributions along the adhesive bondline, were plotted in Figure 6. The results are presented for a given scarf angle of 3°. It can be observed that as the number of plies increases, the peak stresses decrease near the bondline ends. An important factor can explain these results: as the number of plies increases, the number of (0/90) plies in the facesheet is increasing, so the proportion of the stress carried in the outer-most (0/90) plies decreases. This results in lower peak stresses in the adhesive bondline. The same results were found by Gunnion et al [13] for monolithic scarf bonded repairs.

4.3.2 *Failure Load*

Figure 7 compares the ultimate stress obtained for the repair made on skins of different thicknesses. It can be observed that the ultimate stress increases with the increase of the skin thickness. One of the reasons is that when increasing the number of plie, the number of (0/90) plies in the facesheet is increasing, so we reduce the stress peaks in the bondline. The higher strength recovery is for the thicker facesheet. Similar results were obtained also for bonded repair on monolithic composite laminates [16]. For the 2-ply and the 4-ply skin models, failure occurs in the adhesive bondline. However, for the thicker skin (8-ply skin), failure occurs no more in the adhesive bondline but in the composite plies.

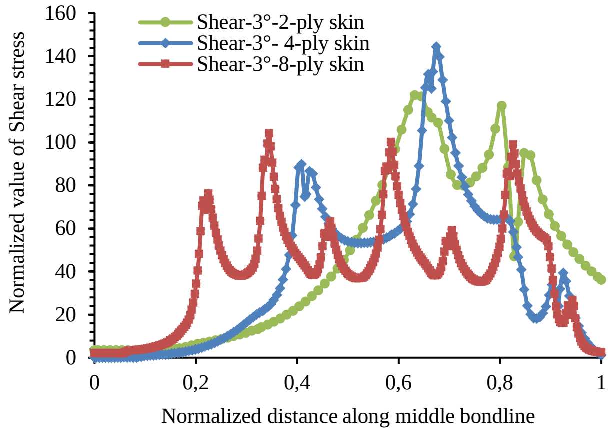

(a) Shear stress distribution

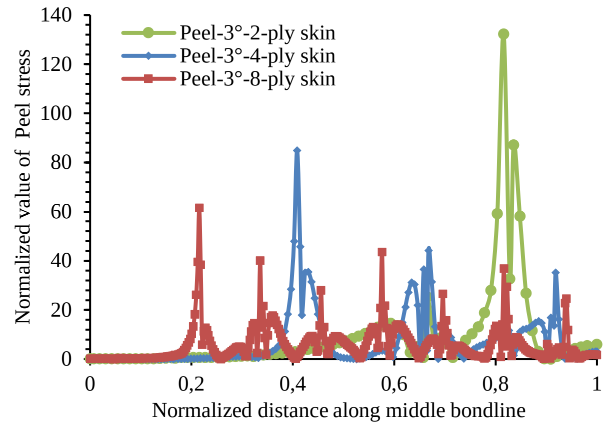

(b) Peel stress distribution

Figure 6 : Shear and peel stresses distributions as a function of number of plies in the adhesive bondline for 3° repaired panels

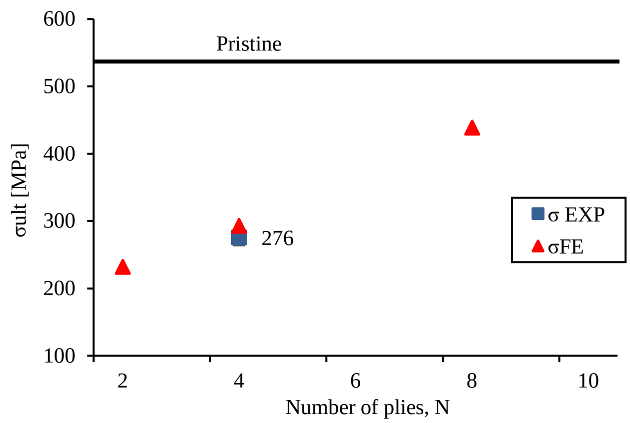

Figure 7 : Repair strength prediction as function of the number of plies (α=3°)

5 CONCLUSION

This study presented an investigation of the influence of geometric parameters (scarf angle, overply overlap length, number of plies) on the stresses distribution along the adhesive bondline and on the ultimate tensile stress. Linear elastic model and non-linear elastoplastic model were generated in order to conduct this parametric study. Results showed that the shear and peel peak stresses are very sensitive to scarf angle, to the addition of an overply and to the number of plies. The addition of an overply provides a good protection for the free edges of the adhesive and increases the strength recovery to about 90%. Results from experimental tests were used to validate the numerical results obtained from the simulation and a good correlation was found.

ACKNOWLEDGEMENT

We would like to thank the Natural Sciences and Engineering Research Council of Canada (NSERC), the Consortium for Research and Innovation in Aerospace in Quebec (CRIAQ), the National Research Council Canada (NRC), Bombardier Aerospace and L3-MAS for funding, technical support and materials.

6 REFERENCES

[1] S. Mahdi, A. J. Kinloch, F. L. Matthews, and M. A. Crisfield, "The Static Mechanical Performance of Repaired Composite Sandwich Beams: Part I - Experimental Characterization," *J. Sandw. Struct. Mater.*, vol. 5, no. 2, pp. 179–202, Apr. 2003.

[2] S. Mahdi, A. J. Kinloch, F. L. Matthews, and M. A. Crisfield, "The Static Mechanical Performance of Repaired Composite Sandwich Beams: Part II - Finite Element Modelling," *J. Sandw. Struct. Mater.*, vol. 5, no. 3, pp. 267–303, Jul. 2003.

[3] S. Mahdi, A. J. Kinloch, and M. A. Crisfield, "Fatigue performance of undamaged and repaired composite sandwich beams," pp. 229–247, 2003.

[4] D. A. Ramantani, R. D. S. G. Campilho, M. F. S. F. D. Moura, and A. T. Marques, "Stress and Failure Analysis of Repaired Sandwich Composite Beams using a Cohesive Damage Model," *J. Sandw. Struct. Mater.*, vol. 12, no. 3, pp. 369–390, May 2010.

[5] S. Liu, Z. Guan, X. Guo, K. Sun, and J. Kong, "Edgewise compressive performance of repaired composite sandwich panels – Experiment and finite element analysis," *J. Reinf. Plast. Compos.*, vol. 32, no. 18, pp. 1331–1347, Sep. 2013.

[6] J. S. Tomblin, L. Salah, J. M. Welch, and B. Michael D., "Bonded Repair of Aircraft Composite Sandwich Structures," Washington, DC 20591, Final Report DOT/FAA/AR-03/74, Feb. 2004.

[7] J. S. Tomblin, T. Lacy, and B. Smith, "Review of damage tolerance for composite sandwich airframe structures.," Washington, Final Report DOT/FAA/AR-99/49, Aug. 1999.

[8] T. Zhang, Y. Yan, and C. Jin, "Experimental and Numerical Investigations of Honeycomb Sandwich Composite Panels With Open-hole Damage and Scarf Repair Subjected to Compressive Loads," *J. Adhes.*, vol. 92, no. 5, pp. 380–401, May 2016.

[9] *Abaqus/ Standard 2004. User Manuel, User Subroutines & Parametric Studies, Vol.VII, Version 6.* .

[10] E. Ghazali, M. Dano, A. Gakwaya, and C.-O. Amyot, "Mechanical performance of repaired sandwich panels: Experimental characterization and finite-element modelling," *Journal of Sandwich Structures and Materials*, Jan-2017.

[11] K. Bodjona *et al.*, "Design of composite bolted and bonded hybrid joints," presented at the 7th CRIAQ Forum, Montreal, Canada, Apr-2014.

[12] "Euro-Composites Corporation, Certificate of Compliance Honeycomb core, nylon fiber base, phenolic resin coated: ECA-R 4.8-64 (3/16-4.0)." Sep-2012.

[13] A. J. Gunnion and I. Herszberg, "Parametric study of scarf joints in composite structures," *Compos. Struct.*, vol. 75, no. 1–4, pp. 364–376, Sep. 2006.

[14] R. D. S. G. Campilho, M. F. S. F. de Moura, A. M. G. Pinto, J. J. L. Morais, and J. J. M. S. Domingues, "Modelling the tensile fracture behaviour of CFRP scarf repairs," *Compos. Part B Eng.*, vol. 40, no. 2, pp. 149–157, Mar. 2009.

[15] H. Bendemra, P. Compston, and P. J. Crothers, "Optimisation study of tapered scarf and stepped-lap joints in composite repair patches," *Compos. Struct.*, vol. 130, pp. 1–8, Oct. 2015.

[16] J. Li, Y. Yan, Z. Liang, and T. Zhang, "Experimental and Numerical Study of Adhesively Bonded CFRP Scarf-Lap Joints Subjected to Tensile Loads," *J. Adhes.*, vol. 92, no. 1, pp. 1–17, Jan. 2016.